Research Article

Production of chitosan scaffolds by lyophilization or electrospinning: which is better for peripheral nerve regeneration?

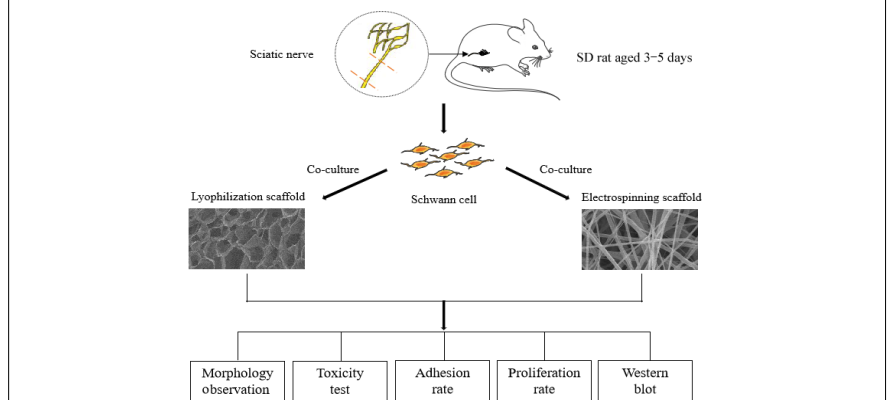Yu-Xuan Wu[1, #], Hao Ma[2, #], Jian-Lan Wang[3], Wei Qu[1, *]

Graphical Abstract *Comparison of Schwann cells growing on lyophilization and electrospinning scaffolds*

Abstract

Both lyophilization and electrospinning are commonly used to make chitosan scaffolds. However, it remains unknown which method is better for cell growth. In this study, we established the following groups: (1) lyophilization group—chitosan scaffolds were prepared by lyophilization method and seeded with Schwann cells from Sprague-Dawley rats aged 3–5 days; (2) electrospinning group—chitosan scaffolds were prepared by electrospinning method and seeded with Schwann cells; (3) control group—Schwann cells were cultured on culture dishes. The growth of Schwann cells was evaluated by immunofluorescence and scanning electron microscopy. Western blot assay was performed to explore the mechanism of Schwann cell growth. Both materials were non-toxic and suitable for the growth of Schwann cells. The pores produced by electrospinning were much smaller than those produced by lyophilization. The proliferation rate and adhesion rate of Schwann cells in the electrospinning group were higher than those in the lyophilization group. Schwann cells cultured on electrospinning scaffolds formed a Bungner band-like structure, and a much greater amount of brain-derived neurotrophic factor was secreted, which can promote the growth of neurons. Our findings show that the chitosan scaffold prepared by the electrospinning method has a nanofiber structure that provides an extracellular matrix that is more favorable for cell-cell interactions. The electrospinning method is more suitable for nerve regeneration than the lyophilization method. This research was approved by the Medical Ethical Committee of Dalian Medical University (approval No. AEE1-2016-045) on March 3, 2016.

Key Words: cells; factor; growth; *in vitro*; model; peripheral nerve; plasticity; protein; rat; regeneration

Chinese Library Classification No. R459.9; R363; R364

Introduction

With the development of neural tissue engineering, artificial scaffolds have been widely used to bridge peripheral nerve defects (Li et al., 2018a; Rao et al., 2019). Biocompatibility between the biomaterial and living cells is essential for an effective tissue engineered nerve graft. Artificial scaffolds are needed for mechanical support and to recreate an environment conducive to cell attachment and proliferation. Chitosan, a derivative of chitin, is a natural material that is mainly composed of N-glucosamine. Because of its excellent biodegradability, antibacterial activity and non-toxicity, chitosan is a wonderful biomaterial for neural tissue engineering for treating peripheral nerve injury (Wang et al., 2016; Li et al., 2018a; Zhang et al., 2018).

Various cell types have been seeded onto artificial scaffolds for treating never injury (Merolli et al., 2019; Onesto et al., 2020). Schwann cells (SCs) are the most commonly used seed cells, and can promote the growth of the axon, stimulate remyelination and reduce the formation of cysts (Deng et al., 2015). Animal studies show that chitosan scaffolds transplanted with SCs produce satisfactory results in repairing the nerve defect (Carvalho et al., 2018; Zhu et al., 2018). Traditionally, lyophilization was usually used in the preparation of chitosan scaffolds (Ariani et al., 2013; Xiao et

[1]Department of Hand Microsurgery, First Affiliated Hospital of Dalian Medical University, Dalian, Liaoning Province, China; [2]Department of Plastic and Reconstructive Surgery, Shanghai Ninth People's Hospital, School of Medicine, Shanghai Jiao Tong University, Shanghai, China; [3]Department of Traditional Chinese Medicine, First Affiliated Hospital of Dalian Medical University, Dalian, Liaoning Province, China
*Correspondence to: Wei Qu, PhD, dlquweidoc@hotmail.com.
https://orcid.org/0000-0002-0069-7472 (Wei Qu)
#Both authors contributed equally to this manuscript.

al., 2019). Scaffolds made in this manner have the benefit of increasing the contact area because of high porosity. SCs can easily adhere to these scaffolds. However, several investigators have proposed that artificial scaffolds should have the ability to promote the directional guidance of regenerating axons and migrating SCs. The electrospinning method generates a scaffold with a nanostructure and high porosity (Teo and Ramakrishna, 2006; Liu et al., 2017; Sandri et al., 2019). With this method, the scaffolds can provide an aligned extracellular matrix for the oriented growth of SCs and axons. Both lyophilization and electrospinning are favorable methods for the preparation of chitosan scaffolds. However, to our knowledge, the relationship between the substrate microstructure and SC characteristics remains unknown.

In this study, we used lyophilization and electrospinning to prepare chitosan scaffolds, and investigated their microstructure and toxicity, and the proliferation and adhesion of SCs. The morphology of SCs growing on the scaffold was assessed by immunofluorescence and scanning electron microscopy. Western blot assay was used to compare the secretion of S100 and brain-derived neurotrophic factor (BDNF), which are associated with the biological activity of SCs. Our aim was to compare the biological characteristics of the scaffolds prepared by the two techniques after co-culture with SCs, and to determine which technique is more suitable for SC growth. Probing these physically-induced biochemical changes in SCs may contribute to optimizing the application of nerve tissue engineered scaffolds.

Materials and Methods

Animals
Twenty male Sprague-Dawley rats, aged 3–5 days and weighing 5–10 g, were included in this study. All the rats were supplied by the Specific-Pathogen-Free Animal Laboratory of Dalian Medical University, China (license No. SCXK (Liao) 2008-0002). This research was approved by the Medical Ethical Committee of Dalian Medical University (approval No. AEE1-2016-045) on March 3, 2016.

Group assignment
To compare the morphology, proliferation rates, adhesion rates and protein levels of SCs, the following three groups were established: (1) lyophilization group, in which chitosan scaffolds were prepared by the lyophilization method and implanted with SCs; (2) electrospinning group, in which chitosan scaffolds were prepared by the electrospinning method and implanted with SCs; (3) control group, in which SCs were cultured on culture dishes.

To evaluate the toxicities of the scaffolds, the toxicities of the scaffold leachates were compared by CCK8 assay. The leachate was then diluted into four different concentrations, and seven groups were established, including (1) 100% electrospinning group: 10% fetal bovine serum (FBS) in electrospinning primary leachate; (2) 50% electrospinning group: 10% FBS and 40% Dulbecco's modified Eagle's medium (DMEM) in electrospinning primary leachate; (3) 25% electrospinning group: 10% FBS and 65% DMEM in electrospinning primary leachate; (4) 100% lyophilization group: 10% FBS in lyophilization primary leachate; (5) 50% lyophilization group: 10% FBS and 40% DMEM in lyophilization primary leachate; (6) 25% lyophilization group: 10% FBS and 65% DMEM in lyophilization primary leachate; (7) control group: 10% FBS in DMEM. Purified SCs were added to each group of leachate to prepare cell suspensions at 5×10^4 cells/mL.

Lyophilization
The chitosan (medium molecular weight; Sigma-Aldrich, St. Louis, MO, USA) was fully dissolved in 1% acetic acid (First Hospital of Dalian Medical University, > 99.5%) by magnetic stirrer. The bubbles were ultrasonically removed, and the concentration was 2% w/v. The chitosan solution was poured into the mold and frozen at −20°C for 4 hours. The frozen materials were disposed in the freeze dryer (Dalian University, China) for 12 hours to completely sublimate the water in the material to maintain the pore structure in the chitosan scaffold. Next, the material was placed in a 5% sodium hydroxide solution for 20 minutes to neutralize the acetic acid molecules. Finally, the material was frozen again for 12 hours, and the chitosan material displayed a porous structure.

Electrospinning
The chitosan was dissolved in 1% w/v hexafluoroisopropanol (52517 MSDS; Sigma-Aldrich) at 37°C for 24–48 hours. After it was completely dissolved, the solution was poured into a syringe and mounted on a flow pump (First Hospital of Dalian Medical University). The spinning conditions were set to a voltage of 15 kV, a nozzle and aluminum foil at a distance of 10 cm, a flow rate of 1 mL/h, a temperature of 25°C, a humidity of less than 35%, and a spinning time of 2 hours. The chitosan was collected on a foil as a white round film with a thick central edge.

Comparison of the microstructure on different scaffolds by scanning electron microscopy
Scaffolds were sprayed with gold, and the surface morphology of the material was observed by scanning electron microscopy (Dalian University of Technology, China). The size of the voids in the lyophilization group and the fiber diameter of the electrospinning group were measured by Photoshop, and the void width distribution was calculated.

Isolation and purification of SCs
The sciatic nerve was excised from rats and enzymatically dissociated with 1% collagenase and 0.125% trypsin. The mixture was triturated, centrifuged, and resuspended in 10% FBS (Thermo Fisher Scientific, Waltham, MA, USA) in DMEM (Thermo Fisher Scientific) for 24 hours. Afterwards, cytosine arabinoside (C3350000 MSDS; Sigma-Aldrich) was added and incubated for an additional 48 hours to remove fibroblasts. Subsequently, the cells were cultured in DMEM supplemented with 10% FBS, forskolin and heregulin for proliferation (Gu et al., 2014).

Comparison of SCs seeded on different scaffolds by scanning electron microscopy
The morphology of SCs on the lyophilization and electrospinning scaffolds after 3 days of culture was observed. Scaffolds were soaked in 95% ethanol overnight, irradiated with ultraviolet light for 1 hour, washed three times with PBS solution, and then immersed in low-sugar DMEM containing 10% high-quality fetal bovine serum for 2 hours. They were cut into 1 cm × 1 cm flakes, placed on the bottom of a 24-well plate, and implanted with SCs at 5×10^4 cells/mL. The SCs were cultured for 3 days. The scaffolds and cells were fixed with paraformaldehyde and sprayed with gold after drying, and then observed by scanning electron microscopy (Carl Zeiss, Germany).

Comparison of SCs in different scaffolds by immunofluorescence microscopy
In the lyophilization and electrospinning groups, the scaffolds were cultured with cells for 3 days. In the control group, the SCs were transferred to culture dishes and cultured for 3 days. Then, all samples were fixed with paraformaldehyde, and rinsed with 0.01 M PBS. Thereafter, 0.2% Triton X-100 (Sigma), 50 μL, was added to the scaffolds. After permeabilization for 5–10 minutes, the samples were rinsed again, and treated with 1% bovine serum albumin (Sigma), 50 μL, for 20 minutes. The samples were incubated with S100 rabbit anti-mouse primary antibody diluted in PBS (1:100), 20 μL, overnight in a 4°C wet box. The slides were then rinsed with PBS and treated with bovine serum albumin. FITC-labeled secondary antibody

(goat anti-rabbit IgG), 20 μL, was then added and incubated in the dark for 1 hour. DAPI staining was conducted after a PBS rinse. Images were captured under a fluorescence microscope (E-200, Nikon, Tokyo, Japan).

Comparison of the toxicity of scaffold leachates by CCK8 assay

The SCs were cultured with leachate for 1, 3, 5 or 7 days, and toxicity was tested by CCK8 assay. The optical density (OD) value of the cells was recorded. Preparation of leachate was as follows: scaffolds were soaked in 75% alcohol for 48 hours, and under an ultraviolet lamp for 12 hours. Then, the cells were immersed in serum-free DMEM at 37°C for 72 hours, and finally placed in a refrigerator at 4°C for later use. The ratio of material to DMEM was 0.1 g/mL. Primary leachates in the lyophilization and electrospinning groups were prepared by soaking with the respective scaffold. The leachates were prepared into four different concentrations, which were then used to produce the seven groups described above.

Cell suspensions were sequentially added to a 96-well plate, 200 μL (1×10^4 cells) per well, with 5 wells per group, and then cultured in the incubator. After 1, 3, 5 or 7 days, 20 μL CCK8 (0.1 mg/mL; Thermo Fisher Scientific) reagent was added into each well, and cultured for 2 hours. The OD value was calculated following enzyme-linked assay. Relative growth rate (RGR, %) was calculated as follows: (OD value in the experimental group / OD value in the control group) × 100%. The toxicity rating of the material was evaluated based on the RGR value. Evaluation criteria were as follows: RGR ≥ 100% is level 0; RGR = 75–99% is level 1; RGR = 50–74% is level 2; RGR = 25–49% is level 3; RGR = 1–24% is level 4; RGR = 0 is level 5. Level 0 or 1 is qualified; level 2 should be evaluated with cell morphology; level 3–5 is unqualified.

Comparison of the proliferation of SCs on different scaffolds by CCK8 assay

The proliferation of SCs on scaffolds was tested after 3 days of culture. Scaffolds were cut into 1 cm × 1 cm pieces (thickness of 0.5 mm) and soaked in 75% alcohol for 48 hours. They were then laid flat on the bottom of a 96-well plate to ensure the films entirely covered the bottom of the well. SCs were digested to prepare 40×10^3 cells/mL cell suspensions, and equal amounts of cell suspension were added to the wells and incubated for 3 days. Finally, CCK8 20 μL was added for detection. The OD value, indicative of cell proliferation on the scaffolds, was measured. The proliferation rate was calculated as follows: (OD value in the lyophilization/electrospinning group / OD value in the control group) × 100%.

Comparison of cell adhesion on scaffolds

The adhesion of SCs on the scaffolds was tested after 2, 6, 12 and 24 hours of culture. Scaffolds were cut into 1.5 cm × 1.5 cm pieces (thickness of 0.5 mm) and soaked in 75% alcohol for 48 hours, and then laid on the bottom of a 6-well plate. Thereafter, 1 mL of cell suspension (1×10^4 cells/mL) was added to each well, and equal amounts of suspension was added to an additional 6-well plate without scaffold as a control group. After culture for 2, 6, 12 or 24 hours, the cells were removed by washing the plate three times with PBS, and the cells were digested by trypsinization to prepare cell suspensions. Finally, the cells were counted in each well. Cell adhesion rate (%) was calculated as follows: (number of adherent cells / 10,000) × 100%.

Western blot assay

BDNF is one of many neurotrophins in the brain that help stimulate and regulate neurogenesis. S100 protein is the most widely used marker of the peripheral nerve sheath and SCs. The levels of BDNF (0.1 μg/mL dilution, rabbit/IgG, polyclonal; Thermo Fisher Scientific) and S100 (1–3 μg/mL dilution, mouse/IgG2a, monoclonal; Thermo Fisher

Scientific) were verified by western blot assay after 3 days of culture. Proteins from SCs were extracted with RIPA buffer (PMSF:RIPA = 1:100; Solarbio Science Technology, Beijing, China). Protein lysates were separated on 8–12% SDS-PAGE gels. The proteins were transferred to polyvinylidene fluoride membranes by electrophoretic transfer. The primary antibody (1:800–1:1000) was diluted with 5% skimmed milk according to the instructions and incubated overnight in a shaker at 4°C. Horseradish peroxidase-labeled secondary antibody (IgG, rabbit and mouse, 1:3000–1:5000) was diluted with antibody diluent and incubated at room temperature for 1 hour. Blots were developed with the chemiluminescence system, and the bands were measured by ImageJ software (National Institutes of Health, Bethesda, MD, USA).

Statistical analysis

Statistical analysis was performed using SPSS 16.0 software (SPSS, Chicago, IL, USA). Data are presented as the mean ± SD. Comparisons between two groups were performed with Student's *t*-test. One-way analysis of variance followed by the Tukey–Kramer *post hoc* test, and two-way analysis of variance with repeated measures were used to evaluate the statistical significance among the three groups. A value of $P < 0.05$ was considered statistically significant.

Results

Microstructure of the scaffolds

Scaffolds prepared by lyophilization had a porous structure. The average size of the pore was 10,185.36 ± 5402.44 μm^2, with a diameter of 50–200 μm (**Figure 1A**). The electrospinning scaffolds had a nanofiber structure, with a mean size of 55.57 ± 28.54 μm^2, and a fiber diameter of 0.2–2 μm (**Figure 1B**). Both types had a uniform microstructure. However, lyophilization mainly produced sponge-like pores, while the electrospun scaffolds had nanofibers with a criss-cross arrangement. The surface of the electrospinning scaffolds was aligned.

Characterization of SCs cultured on the scaffolds

SCs displayed clustered growth in both scaffolds by scanning electron microscopy. In the lyophilized scaffold, the cells were distributed in the voids (**Figure 1C** and **D**), whereas they adhered to the surface of the nanofibers in the electrospun scaffolds (**Figure 1E** and **F**). By immunofluorescence for S100, the SCs were well-distributed on the electrospinning scaffolds and were growing and proliferating uniformly. In comparison, the SCs clustered together in the voids of the lyophilization scaffolds. The distribution of the cells was uneven and not on the same plane of the scaffolds. In the control group, SCs cultured without a scaffold grew in a disordered manner (**Figure 1G–I**). In co-cultures of Schwann cells and scaffolds, the morphology of Schwann cells was not significantly different between the two groups by microscopy.

Safety evaluation

The OD value of cell proliferation in each leachate group gradually increased at 1, 3, 5 and 7 days (**Figure 2A**). There were no significant differences among the groups ($P > 0.05$). The RGR values of the two different scaffold types at each time point were between 90% and 110%, showing that both were conducive to SC growth (**Figure 2B** and **Tables 1**, **2**).

Proliferation and adhesion of SCs on the scaffolds

The mean proliferation rate was 102.49 ± 5.07% in the lyophilization group and 129.67 ± 1.24% in the electrospinning group, with a significant difference between them ($P < 0.001$). The electrospinning group had a higher proliferation rate (**Figure 2C** and **Table 3**). Over time, more cells adhered to both scaffolds. After 24 hours, the adhesion rate was 39.11 ± 2.53% in the lyophilization group and 63.01 ± 3.23% in the electrospinning group. The difference between the two groups

Research Article

was significant (P < 0.001), with the electrospinning group having a higher adhesion rate (**Figure 2D** and **Table 4**).

Expression of growth-related proteins by Schwann cells on the scaffolds

Western blot assay showed that S100 and BDNF protein levels in the lyophilization and electrospinning groups were both significantly increased compared with the control group. For S100: control *vs*. lyophilization, P = 0.0067; control *vs*. electrospinning, P = 0.0139; lyophilization *vs*. electrospinning, P = 0.0374. For BDNF: control *vs*. lyophilization, P = 0.0395; control *vs*. electrospinning, P = 0.0105; lyophilization *vs*. electrospinning, P = 0.0346 (**Figure 3**).

Discussion

Based on previous studies, the ideal tissue engineering material should have the following characteristics: good biodegradability, biocompatibility, three-dimensional structure, good mechanical properties, and conducive to cell adhesion and proliferation (Larsen et al., 2006; Benhabbour et al., 2008; Sofi et al., 2018; Ranganathan et al., 2019). Chitosan is a derivative of chitin, which is a natural material mainly composed of N-glucosamine. It is widely used in the field of biomedicine because of its excellent biocompatibility, biodegradability, absorbability, antibacterial activity, anticoagulant activity, and ability to promote wound healing (Senel and McClure, 2004; Li et al., 2018b). Chitosan has been seeded with Schwann cells, chondrocytes and epidermal cells to treat peripheral nerve injury (Keilhoff et al., 2006; de Ruiter et al., 2009; Li et al., 2017; Boecker et al., 2019), spinal cord injury (Li et al., 2009; Boido et al., 2019), articular surface damage (Montembault et al., 2006), skin defects (Mi et al., 2001) and other diseases (Whu et al., 2013). Our current findings show that chitosan scaffolds prepared by lyophilization and electrospinning provide good biomechanical support.

SCs are the most important glial cells, and play critical roles in stimulating axonal growth and reducing cyst formation (Deng

et al., 2015; Jessen and Mirsky, 2016; Clervius et al., 2019; Torii et al., 2019). When damage occurs to the peripheral nerve, SCs assist in the organization of the neural extracellular matrix, participate in the myelination of regenerating axons, provide structural support for axon regeneration, and supply nutrients. Previous animal studies have already demonstrated the beneficial effects of SC transplantation for peripheral nerve defects. Moreover, the role of SCs in promoting axon regeneration was shown using a chitosan conduit (Zhu et al., 2018).

In our study, two protocols were used to engineer nerve scaffolds for culturing SCs, and both methods provided a perfect growth environment. The principle of the lyophilization method is to freeze the plastic solution and then sublimate the solvent under vacuum to retain the solute, thereby producing a scaffold with a void structure (Ariani et al., 2013; Pisano et al., 2019). The structure of the lyophilization scaffold is sponge-like, which has the advantage of increasing contact area and porosity. In the electrospinning method, the material is processed into a jet stream with an electrostatic charge under the action of an applied high-voltage electric field force, and is collected by the receiver and dried to obtain a material with a nanofiber structure (Senel and McClure, 2004). The materials prepared by this method have a nanometer structure, a fiber network, a large specific surface area and high porosity (Teo and Ramakrishna, 2006). As seen from the scanning electron microscopy images, the lyophilization chitosan scaffold has a 50–200 μm uniform pore structure, while the electrospinning scaffold has a 0.2–2-micron uniform nanoscale fiber structure. Both scaffolds stimulate the growth of SCs, but to different degrees, mainly because the microenvironment provided by the two structures to Schwann cells is significantly different.

Scaffolds seeded with SCs were examined by immunofluorescence and scanning electron microscopy to assess biocompatibility. The results provide an important basis for further applications of the two techniques in tissue engineered nerve scaffolds. The leachate toxicity assay showed that the different leachates had similarly low toxicity. The proliferation assay showed that the electrospinning scaffold was significantly better than the lyophilization scaffold in supporting cell division. This might be because the electrospun scaffold has a better microstructure, with reticulated nanostructures that provide better support for SCs. The adhesion assay showed that electrospun scaffolds retain more adherent cells. Together, these results show that the electrospinning of nanofibers allows for a connected and porous scaffold, which can mimic the extracellular matrix structurally, chemically and mechanically (Ladd et al., 2011).
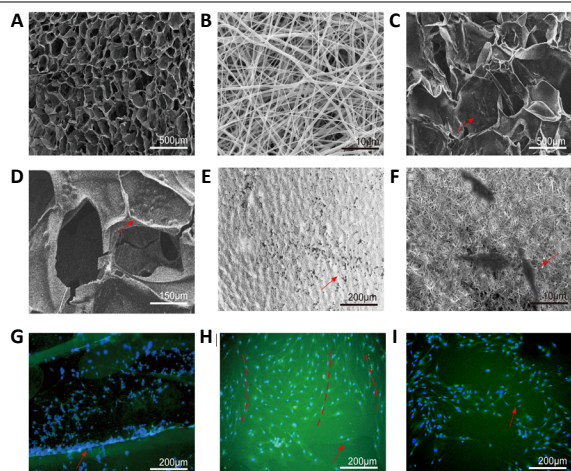
Figure 1 | Observation by scanning electron microscopy and fluorescence microscopy.
(A) Surface morphology of the lyophilization scaffold. (B) surface morphology of the electrospinning scaffold. (C, D) Schwann cells (SCs) were cultured on the lyophilization scaffold, and the cells clustered together in the voids. (E, F) SCs were cultured on electrospinning scaffold, and the cells adhered to the surface of the nanofibers. (A–F) SCs were observed by scanning electron microscopy. (G) Immunofluorescence S100 staining of SCs on a lyophilization scaffold. The distribution of the cells was uneven and not on the same plane of the scaffolds. (H) Immunofluorescence S100 staining of SCs on an electrospinning scaffold. SCs were well-distributed and grew in sequence (red dotted line). (I) SCs cultured without a scaffold grew in a disordered manner. (G–I) SCs were observed under a fluorescence microscope: Blue represents the nucleus and green represents cytoplasm. Red arrows point to SCs.
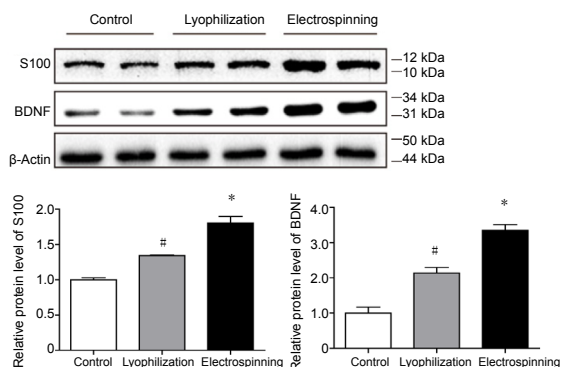

Figure 3 | Western blot assay for S100 and BDNF after 3 days of culture.
Western blot assay of protein levels of S100 and brain-derived neurotrophic factor (BDNF) in each group and quantification. The S100 and BDNF protein levels in both lyophilization and electrospinning groups were significantly increased compared with the control group. *$P < 0.05$, vs. lyophilization group; #$P < 0.05$, vs. control group. Data are expressed as the mean ± SD ($n = 5$; one-way analysis of variance followed by the Tukey-Kramer post hoc test).

In a chitosan scaffold prepared by lyophilization, the pore diameter is larger, and the cells grow in clusters in the pores. The poor penetrability of the pores reduces contact with clustered SCs in other pores. The diameter of nanofibers in the electrospun structure is smaller than that of the cells, and SCs show a tendency for planar growth on the material. The cell poles are fully fused with the fiber structure, and the distribution of cells is relatively more uniform, which is beneficial to the interaction of the SC clusters. Furthermore, the SCs are able to align to form a Bungner band-like structure, which can direct axon regrowth to the target and are indispensable for nerve repair (Jessen and Mirsky, 2016).

Previous studies show that a favorable extracellular matrix can mediate cell interactions in an optimal manner. Not only the biochemical substances, but also physical interactions affect cell behaviors and their internal environment (Guilak et al., 2009; Teixeira et al., 2009; Gilbert et al., 2010; Hughes
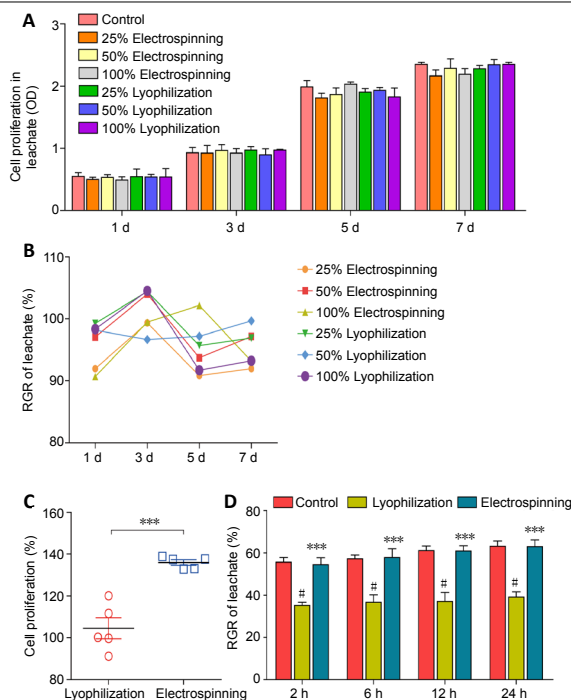
Figure 2 | Relative growth rate, cell proliferation and cell adhesion.
(A) Comparison of the toxicity of leachates of the scaffolds by CCK8 assay: The OD values representing SC proliferation in each leachate were not significantly different at 1, 3, 5 or 7 days ($P > 0.05$, two-way analysis of variance with repeated measures). (B) RGR of leachate at 1, 3, 5 and 7 days. RGR ranged from 90% to 110%. (C) Proliferation rate of SCs on the electrospinning scaffold was greater than that on the lyophilization scaffold (***$P < 0.001$, vs. lyophilization group; Student's t-test). (D) Adhesion rate of SCs on the electrospinning scaffold was higher than that on the lyophilization scaffold, and there was no significant difference between the electrospinning group and the control group. ***$P < 0.001$, vs. lyophilization group; #$P < 0.05$, vs. control group. Data are expressed as the mean ± SD ($n = 5$; two-way analysis of variance with repeated measures). OD: Optical density; RGR: relative growth rate; SCs: Schwann cells.

and Nibbs, 2018). Various cells, such as fibroblasts, articular chondrocytes, muscle cells, smooth muscle cells and bone marrow mesenchymal stem cells, are significantly affected by the physical properties of the extracellular matrix. Previous studies show that SC adhesion is affected by the stiffness and elasticity of the extracellular matrix (Pek et al., 2010; Gu et al., 2012). Western blot assay results showed that adhesion-related proteins are significantly differently expressed. Furthermore, differences in the microtopography of the scaffolds significantly affects cellular adhesion, activation and gene expression (Thery et al., 2006; Bashur et al., 2009). For example, scaffolds with a nanofiber structure distinctly promote chondrogenic redifferentiation and growth compared with lyophilization scaffolds, as demonstrated by reverse transcription-polymerase chain reaction and western blot assay (Noriega et al., 2012). Different fiber diameters also differentially influence gene expression. Internal stress is generated among cells because of the attachment to the nanofibers, which retain more non-adherent cell borders (Geiger et al., 2001; Burute and Thery, 2012).

In the present study, scanning electron microscopy showed different arrangements of SCs on lyophilization and electrospinning scaffolds. Furthermore, western blot assay revealed that the expression levels of BDNF and S-100 were significantly different because of different extracellular matrix structures. S100 expressed in motor and sensory neurons was shown to promote neuronal survival and neurite extension in vitro (Fardell et al., 2018). The increased expression of BDNF can promote the growth of neurons and the elongation of axons. BDNF also promotes a series of neural responses by binding to specific cell surface receptors (Yeung et al.,

2005). A previous FITC-phalloidin study showed that the actin microfilaments exhibited various arrangements on substrates of different stiffness. A favorable stiffness contributed to a conducive internal environment for the expression of various neurotrophic factors (ciliary neurotrophic factor, nerve growth factor, BDNF) and adhesion-related proteins (N-cadherin and β-catenin) by SCs (Ladoux et al., 2010). Our current findings are consistent with these previous studies. A favorable structural extracellular matrix contributes to coordinated cell interactions and a conducive environment.

Although our results show that the microtopography of the extracellular matrix impacts the growth and proliferation of SCs, the molecular mechanisms, including molecular pathways and upstream and downstream regulatory proteins, remain unknown. In future studies, we plan to investigate genomics and proteomics, and clarify the physical properties that affect SC characteristics. These studies should help identify the SC proteins that play key roles in nerve repair mediated by the different scaffolds.

In summary, both the lyophilization and electrospinning scaffolds are non-toxic and permissive to SC growth. However, SCs formed a Bungner band-like structure in the electrospun scaffolds, and much more BDNF and S100 were secreted. The nanofiber structure of chitosan scaffolds produced by electrospinning could be a better matrix for neuroregeneration. The favorable physical structure of the extracellular matrix contributes to coordinated cell-cell interactions and an environment conducive to regeneration. In future experiments, we will make chitosan conduits using these two methods, and assess nerve regeneration using a sciatic nerve injury model on rats for *in vivo* studies so as to clarify the specific molecular mechanism and important signal pathways of chitosan scaffolds involved in nerve regeneration.

References

Ariani MD, Matsuura A, Hirata I, Kubo T, Kato K, Akagawa Y (2013) New development of carbonate apatite-chitosan scaffold based on lyophilization technique for bone tissue engineering. Dent Mater J 32:317-325.

Bashur CA, Shaffer RD, Dahlgren LA, Guelcher SA, Goldstein AS (2009) Effect of fiber diameter and alignment of electrospun polyurethane meshes on mesenchymal progenitor cells. Tissue Eng Part A 15:2435-2445.

Benhabbour SR, Sheardown H, Adronov A (2008) Cell adhesion and proliferation on hydrophilic dendritically modified surfaces. Biomaterials 29:4177-4186.

Boecker A, Daeschler SC, Kneser U, Harhaus L (2019) Relevance and recent developments of chitosan in peripheral nerve surgery. Front Cell Neurosci 13:104.

Boido M, Ghibaudi M, Gentile P, Favaro E, Fusaro R, Tonda-Turo C (2019) Chitosan-based hydrogel to support the paracrine activity of mesenchymal stem cells in spinal cord injury treatment. Sci Rep 9:6402.

Burute M, Thery M (2012) Spatial segregation between cell-cell and cell-matrix adhesions. Curr Opin Cell Biol 24:628-636.

Carvalho CR, Wrobel S, Meyer C, Brandenberger C, Cengiz IF, Lopez-Cebral R, Silva-Correia J, Ronchi G, Reis RL, Grothe C, Oliveira JM, Haastert-Talini K (2018) Gellan Gum-based luminal fillers for peripheral nerve regeneration: an in vivo study in the rat sciatic nerve repair model. Biomater Sci 6:1059-1075.

Clervius H, Baig M, Mahavadi A, Gajavelli S (2019) Human neural stem cell transplants to address multiple pathologies associated with traumatic brain injury. Neural Regen Res 14:1699-1700.

de Ruiter GC, Malessy MJ, Yaszemski MJ, Windebank AJ, Spinner RJ (2009) Designing ideal conduits for peripheral nerve repair. Neurosurg Focus 26:E5.

Deng LX, Walker C, Xu XM (2015) Schwann cell transplantation and descending propriospinal regeneration after spinal cord injury. Brain Res 1619:104-114.

Fardell C, Zettergren A, Ran C, Carmine Belin A, Ekman A, Sydow O, Backman L, Holmberg B, Dizdar N, Soderkvist P, Nissbrandt H (2018) S100B polymorphisms are associated with age of onset of Parkinson's disease. BMC Med Genet 19:42.

Geiger B, Bershadsky A, Pankov R, Yamada KM (2001) Transmembrane crosstalk between the extracellular matrix--cytoskeleton crosstalk. Nat Rev Mol Cell Biol 2:793-805.

Gilbert PM, Havenstrite KL, Magnusson KE, Sacco A, Leonardi NA, Kraft P, Nguyen NK, Thrun S, Lutolf MP, Blau HM (2010) Substrate elasticity regulates skeletal muscle stem cell self-renewal in culture. Science 329:1078-1081.

Gu Y, Ji Y, Zhao Y, Liu Y, Ding F, Gu X, Yang Y (2012) The influence of substrate stiffness on the behavior and functions of Schwann cells in culture. Biomaterials 33:6672-6681.

Gu Y, Zhu J, Xue C, Li Z, Ding F, Yang Y, Gu X (2014) Chitosan/silk fibroin-based, Schwann cell-derived extracellular matrix-modified scaffolds for bridging rat sciatic nerve gaps. Biomaterials 35:2253-2263.

Guilak F, Cohen DM, Estes BT, Gimble JM, Liedtke W, Chen CS (2009) Control of stem cell fate by physical interactions with the extracellular matrix. Cell Stem Cell 5:17-26.

Hughes CE, Nibbs RJB (2018) A guide to chemokines and their receptors. FEBS J 285:2944-2971.

Jessen KR, Mirsky R (2016) The repair Schwann cell and its function in regenerating nerves. J Physiol 594:3521-3531.

Keilhoff G, Goihl A, Stang F, Wolf G, Fansa H (2006) Peripheral nerve tissue engineering: autologous Schwann cells vs. transdifferentiated mesenchymal stem cells. Tissue Eng 12:1451-1465.

Ladd MR, Hill TK, Yoo JJ, Lee SJ (2011) Electrospun Nanofibers in tissue engineering. Nanofibers-production, properties and functional applications. Washington: Wake Forest University School of Medicine, USA.

Ladoux B, Anon E, Lambert M, Rabodzey A, Hersen P, Buguin A, Silberzan P, Mege RM (2010) Strength dependence of cadherin-mediated adhesions. Biophys J 98:534-542.

Larsen CC, Kligman F, Kottke-Marchant K, Marchant RE (2006) The effect of RGD fluorosurfactant polymer modification of ePTFE on endothelial cell adhesion, growth, and function. Biomaterials 27:4846-4855.

Li G, Xiao Q, Zhang L, Zhao Y, Yang Y (2017) Nerve growth factor loaded heparin/chitosan scaffolds for accelerating peripheral nerve regeneration. Carbohydr Polym 171:39-49.

Li G, Xue C, Wang H, Yang X, Zhao Y, Zhang L, Yang Y (2018a) Spatially featured porous chitosan conduits with micropatterned inner wall and seamless sidewall for bridging peripheral nerve regeneration. Carbohydr Polym 194:225-235.

Li J, Cai C, Li J, Li J, Li J, Sun T, Wang L, Wu H, Yu G (2018b) Chitosan-based nanomaterials for drug delivery. Molecules 23:2661-2670.

Li X, Yang Z, Zhang A, Wang T, Chen W (2009) Repair of thoracic spinal cord injury by chitosan tube implantation in adult rats. Biomaterials 30:1121-1132.

Liu Y, Wang S, Zhang R (2017) Composite poly (lactic acid)/chitosan nanofibrous scaffolds for cardiac tissue engineering. Int J Biol Macromol 103:1130-1137.

Merolli A, Mao Y, Voronin G, Steele JAM, Murthy NS, Kohn J (2019) A method to deliver patterned electrical impulses to Schwann cells cultured on an artificial axon. Neural Regen Res 14:1052-1059.

Mi FL, Shyu SS, Wu YB, Lee ST, Shyong JY, Huang RN (2001) Fabrication and characterization of a sponge-like asymmetric chitosan membrane as a wound dressing. Biomaterials 22:165-173.

Montembault A, Tahiri K, Korwin-Zmijowska C, Chevalier X, Corvol MT, Domard A (2006) A material decoy of biological media based on chitosan physical hydrogels: application to cartilage tissue engineering. Biochimie 88:551-564.

Noriega SE, Hasanova GI, Schneider MJ, Larsen GF, Subramanian A (2012) Effect of fiber diameter on the spreading, proliferation and differentiation of chondrocytes on electrospun chitosan matrices. Cells Tissues Organs 195:207-221.

Onesto V, Accardo A, Vieu C, Gentile F (2020) Small-world networks of neuroblastoma cells cultured in three-dimensional polymeric scaffolds featuring multi-scale roughness. Neural Regen Res 15:759-768.

Pek YS, Wan AC, Ying JY (2010) The effect of matrix stiffness on mesenchymal stem cell differentiation in a 3D thixotropic gel. Biomaterials 31:385-391.

Pisano R, Arsiccio A, Capozzi LC, Trout BL (2019) Achieving continuous manufacturing in lyophilization: Technologies and approaches. Eur J Pharm Biopharm 142:265-279.

Ranganathan S, Balagangadharan K, Selvamurugan N (2019) Chitosan and gelatin-based electrospun fibers for bone tissue engineering. Int J Biol Macromol 133:354-364.

Rao F, Yuan Z, Li M, Yu F, Fang X, Jiang B, Wen Y, Zhang P (2019) Expanded 3D nanofibre sponge scaffolds by gas-foaming technique enhance peripheral nerve regeneration. Artif Cells Nanomed Biotechnol 47:491-500.

Sandri G, Rossi S, Bonferoni MC, Miele D, Faccendini A, Del Favero E, Di Cola E, Icaro Cornaglia A, Boselli C, Luxbacher T, Malavasi L, Cantu L, Ferrari F (2019) Chitosan/glycosaminoglycan scaffolds for skin reparation. Carbohydr Polym 220:219-227.

Senel S, McClure SJ (2004) Potential applications of chitosan in veterinary medicine. Adv Drug Deliv Rev 56:1467-1480.

Sofi HS, Ashraf R, Beigh MA, Sheikh FA (2018) Scaffolds fabricated from natural polymers/composites by electrospinning for bone tissue regeneration. Adv Exp Med Biol 1078:49-78.

Teixeira AI, Ilkhanizadeh S, Wigenius JA, Duckworth JK, Inganas O, Hermanson O (2009) The promotion of neuronal maturation on soft substrates. Biomaterials 30:4567-4572.

Teo WE, Ramakrishna S (2006) A review on electrospinning design and nanofibre assemblies. Nanotechnology 17:R89-106.

Thery M, Pepin A, Dressaire E, Chen Y, Bornens M (2006) Cell distribution of stress fibres in response to the geometry of the adhesive environment. Cell Motil Cytoskeleton 63:341-355.

Torii T, Miyamoto Y, Yamauchi J (2019) Cellular signal-regulated schwann cell myelination and remyelination. Adv Exp Med Biol 1190:3-22.

Wang TJ, Wang IJ, Hu FR, Young TH (2016) Applications of biomaterials in corneal endothelial tissue engineering. Cornea 35 Suppl 1:S25-30.

Whu SW, Hung KC, Hsieh KH, Chen CH, Tsai CL, Hsu SH (2013) In vitro and in vivo evaluation of chitosan-gelatin scaffolds for cartilage tissue engineering. Mater Sci Eng C Mater Biol Appl 33:2855-2863.

Xiao H, Huang W, Xiong K, Ruan S, Yuan C, Mo G, Tian R, Zhou S, She R, Ye P, Liu B, Deng J (2019) Osteochondral repair using scaffolds with gradient pore sizes constructed with silk fibroin, chitosan, and nano-hydroxyapatite. Int J Nanomedicine 14:2011-2027.

Yeung T, Georges PC, Flanagan LA, Marg B, Ortiz M, Funaki M, Zahir N, Ming W, Weaver V, Janmey PA (2005) Effects of substrate stiffness on cell morphology, cytoskeletal structure, and adhesion. Cell Motil Cytoskeleton 60:24-34.

Zhang L, Zhao W, Niu C, Zhou Y, Shi H, Wang Y, Yang Y, Tang X (2018) Genipin-cross-linked chitosan nerve conduits containing TNF-alpha inhibitors for peripheral nerve repair. Ann Biomed Eng 46:1013-1025.

Zhu C, Huang Y, Xue C, Wang Y, Wang S, Bao S, Chen R, Li Y, Gu Y (2018) Skin derived precursor Schwann cell-generated acellular matrix modified chitosan/silk scaffolds for bridging rat sciatic nerve gap. Neurosci Res 135:21-31.